

PRELIMINARY RESULTS FROM THE ATMOSPHERIC NEUTRAL DENSITY EXPERIMENT RISK REDUCTION MISSION

A.C. Nicholas, J.M. Picone, J. Emmert, J. DeYoung, L. Healy, L. Wasiczko

Naval Research Laboratory

M. Davis

Honeywell TSI

C. Cox

Raytheon Integrated Defense Systems

ABSTRACT

The Atmospheric Neutral Density Experiment (ANDE) Risk Reduction flight was launched on Dec 9, 2006 and deployed into orbit by the Space Shuttle Discovery on December 21, 2006. The primary mission objective is to test the deployment mechanism from the Shuttle for the ANDE flight in mid 2009. Scientific objectives of the ANDE risk reduction flight include: monitor total neutral density along the orbit for improved orbit determination of resident space objects, monitor the spin rate and orientation of the spacecraft, and provide a test object for polarimetry studies.

Each of the two ANDE missions consists of two spherical spacecraft fitted with retro-reflectors for satellite laser ranging (SLR). The ANDE risk reduction mission spacecraft each contain a small lightweight payload designed to determine the spin rate and orientation of the spacecraft from on-orbit measurements and from ground based observations. The follow-on ANDE mission scheduled for launch in 2009 will consist of two spherical spacecraft also fitted with retro-reflectors for SLR. One of these spacecraft will also carry instrumentation to measure the in-situ atmospheric density, composition and winds.

Atmospheric densities derived from observations of the ANDERR spacecraft will be presented and compared to atmospheric models and other data sources. A methodology to improve prediction accuracy by augmenting predictions produced with radar observations with combination radar and satellite laser ranging observations will be presented.

This paper presents a mission overview and emphasis will be placed on the scientific results from the risk reduction mission and a brief overview of the follow-on mission.

INTRODUCTION

Significant advances in the miniaturization of space technology and cost reduction has supported the proliferation of micro satellites. Where once a single satellite contained a suite of instruments to support several mission objectives, often times not all related, current micro satellites are tailored to accomplish a small set of related objectives. Through the use of micro satellite technology, NRL is developing a satellite

suite to improve precision orbit determination and prediction by monitoring total atmospheric density between 300 and 400 km. The suite, known as the Atmospheric Neutral Density Experiment (ANDE)^{1,2}, consists of a series of four micro satellites with instrumentation to perform these interrelated mission objectives. First, provide high quality satellites, with stable and well-determined coefficient of drag, for calibrating techniques and models for precision orbit determination. Second, provide detailed atmospheric composition for validating new ultraviolet remote sensing techniques. Finally, an optical communications experiment using modulating retroreflectors (MRRs) will be conducted during the ANDE mission. The DoD Space Test Program will provide launch services and deployment into orbit for two missions, each mission flying a pair of ANDE spacecraft. The ANDE risk reduction (ANDERR) mission was launched on Dec. 9, 2006 onboard the STS-116, Space Shuttle Discovery, and deployed (as seen in Figure 1) into orbit on Dec. 21, 2006. This paper will focus on the Atmospheric Neutral Density Experiment Risk Reduction (ANDERR)³ flight, which consists of two spherical spacecraft with retro-reflectors for satellite laser ranging (SLR).



S116E07838

Figure 1 The deployment of the Atmospheric Neutral Density Experiment Risk Reduction (ANDERR) spacecraft on December 21, 2006 during the STS-116 mission.

The constant and well-determined cross section and surface properties of the ANDERR spacecraft provide an ideal object for monitoring atmospheric drag. While the exterior of the ANDERR spacecraft determine how well the main science objective is accomplished nothing prohibits the use of the spacecraft's interior space. The interior can be utilized for additional experiments and payloads so long as the interior masses are balanced so that the center of gravity remains at the geometric center. Each of the four spacecraft has their interior populated differently to accommodate respective science goals. One spacecraft in the ANDE mission (launch in 2009) will contain instrumentation to measure the neutral and ion composition directly while the other spacecraft contain the subsystems necessary to measure and/or derive the secondary science objectives.

The primary mission of the ANDE program is to accurately determine the total atmospheric density along the orbit of the spacecraft. The major source of error in determining the orbit of objects in Low Earth Orbit (LEO), altitudes less than 1000 km, is the computation of acceleration due to atmospheric drag. This acceleration is governed by the equation,

$$a_d = -\frac{1}{2}B\rho v^2 \quad (1)$$

where a is the acceleration, ρ is the atmospheric density and v is the orbital velocity relative to the medium. The ballistic coefficient⁴, B , is given by

$$B = \frac{C_D A}{m} \quad (2)$$

with C_D being the coefficient of drag, A the projected frontal area and m the mass of the object.

Several atmospheric density models are routinely used in orbit determination. These include the Jacchia 1970, J70, empirical model derived from satellite observations⁵, the Mass Spectrometer Incoherent Scatter Radar Extended, MSISE-90, model^{6,7} and the recently revised NRLMSISE-00⁸, hereafter referred to as MSIS. The quantity measured with this method is the product of the ballistic coefficient and the total atmospheric density. Hence, to retrieve atmospheric densities from orbital observations one must have adequate knowledge of the ballistic coefficient and the relative velocity of the object with respect to the medium. For example, consider a sphere of known mass in LEO. The cross-sectional area of a sphere is independent of orientation and is therefore constant. Assume the sphere does not have an attitude control system that requires thrusters; therefore the sphere's mass is constant. A high fidelity C_D model can be used to compute the C_D of the sphere for different conditions the sphere will experience in orbit. Inputs to such a model consist of the properties of the surface material of the sphere, surface roughness, the temperature of the sphere, and the temperature and composition of the atmospheric constituents impinging the surface of the sphere^{9,10}. The velocity of the sphere can be obtained from the orbit determination and the velocity of the atmosphere can be modeled using an atmospheric wind model such as the Horizontal Wind Model (HWM)¹¹.

C_D MODELING

A limitation in drag models typically applied in orbit determination software is the lack of modeling for variations in the coefficient of drag (C_D)—which varies independently of the changes in the projected area—as a function of the geometry, and the lack of modeled (as opposed to estimated) cross-track and radial forces. The cross-track and radial forces, in addition to the C_D , change with the incidence angle of the atmospheric flow upon each component area of the spacecraft. Estimation of constant scale factors to the standard formulation for drag (Eq. 1) will not account for this variation, nor will modeling of the projected area. Therefore, we used a modified version of the GEODYN orbit determination software that includes the elemental free molecular flow drag force algorithms of Fredo¹², with modification to the shear and normal force accommodation functions, to model the normal and shear forces acting on each elemental area of the “macro-model”. The molecular mass for the atmospheric flow is provided by the MSIS-86 thermospheric model. In addition, the Horizontal Wind Model 1993 (HWM)¹¹ was implemented. The result is a more realistic drag model that includes the radial and cross-track components of drag, and the variations in C_D with incidence angle. These models were successfully applied to the Tropical Rainfall Measurement Mission and GFZ-1 data⁹.

The ANDERR MAA (and FCal) spacecraft as flown mass and size properties are 52.04 kg (62.70 kg) and 0.1829214 m² (0.1551792 m²)¹³. Each of the ANDERR spacecraft was modeled using 94 flat plates, 73 for the leading hemisphere and 21 for the trailing side, with the computations for momentum accommodation computed for each plate, then aggregated to provide the total C_D . Surface properties for T6

aluminum were assumed, with temperature a surface temperature of 293 K for daylight, and 273K for sunlit conditions. These temperature conditions approximate the measurement data from the active spacecraft.

The C_D for the two spacecraft is shown in Figure 2. The average value for the modeled MAA C_D is 2.1123 with a standard deviation of 0.00763. The average value for the modeled FCal C_D is 2.1113 with a standard deviation of 0.00798. Variation around the orbit is caused by differing atmospheric composition and surface temperature variations. These results are not sensitive to small variations in the plates used. The MAA and FCal spacecraft show the same C_D , despite the differing mass and sphere sizes (which were used in the computations). Differences should appear when the surface composition for each object is considered, the orbits start to separate, and the actual temperature data for each is used.

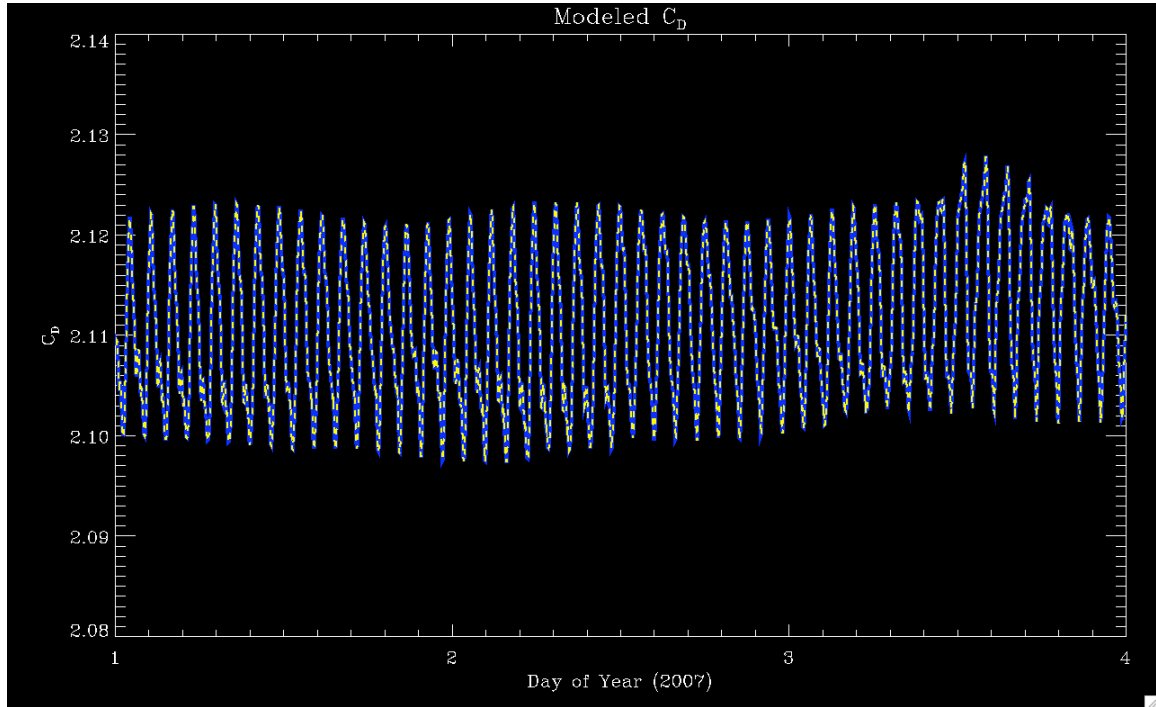


Figure 2 MAA and FCal spacecraft computed C_D using actual orbit, solar flux, and geomagnetic index data.

The C_D for the ANDERR spacecraft were also solved for analytically. The analytic solution¹⁴ for a sphere in free molecular flow is given by:

$$C_D = \frac{(2s^2 + 1)}{\sqrt{\pi}s^3} e^{-s^2} + \frac{(4s^4 + 4s^2 + 1)erf(s)}{2s^4} + \frac{2\sqrt{\pi}(1-\epsilon)}{3s} \sqrt{\frac{T_{sc}}{T_\infty}} \quad (3)$$

where, s is the speed ratio given by

$$s = v \left(2R \frac{T_{sc}}{M_w} \right)^{-1/2} \quad (4)$$

v is the velocity, R is the gas constant, M_w is the molecular weight, T_{sc} is the temperature of the spacecraft surface, T_∞ is the atmospheric temperature, ϵ is the percent of specular reflection, and erf is the error function. Using appropriate values for these parameters an analytic value for the C_D was computed to be

2.10882. This value is quite close (-0.00056%) to the precise numerical integration value computed by NASA JSC for a discretized sphere¹⁵ with 110,536 facets of 2.10881.

SLR OBSERVABILITY

The International Laser Ranging Service (ILRS)¹⁶ performed satellite laser ranging observations of the ANDERR spacecraft. Estimates of the link budget were computed, using an average laser cross section of 0.12 million m², to determine the number of photoelectrons visible by all ILRS stations as a function of elevation angle. The results are presented in Figure 3, where the green symbols represent the MAA spacecraft and the red symbols represent the FCal spacecraft. Figure 4 depicts the measured observations acquired by the SLR ground stations per normal point, plotted in the same format. When provided with accurate predictions there is ample signal returned by the ANDERR retro-reflector arrays for SLR tracking.

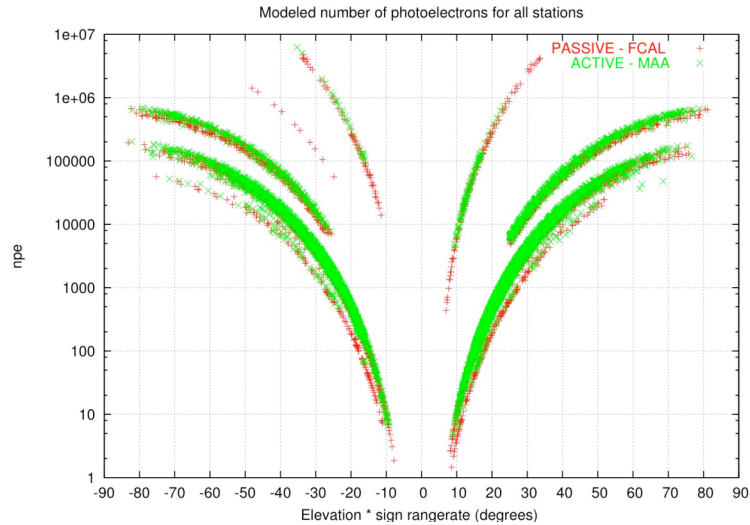


Figure 3 Modeled number of photoelectron returned from the ANDERR spacecraft as a function of product of the elevation angle and the sign of the range rate.

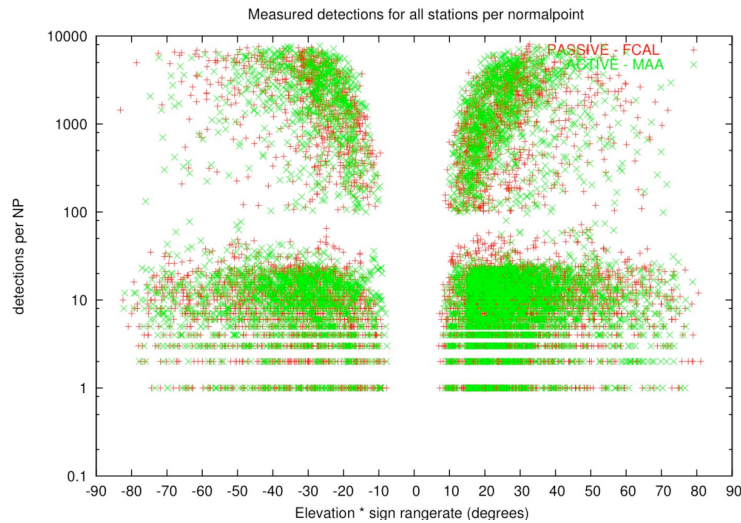


Figure 4 ILRS site measured number of measurements per 5-second interval returned from the ANDERR spacecraft as a function of the product of the elevation angle and the sign of the range rate.

ANDERR DATA FLOW

The 20th Space Control Squadron, USAF in Dahlgren, VA, processes US Space Surveillance Network (SSN) radar observation data of the two ANDERR spacecraft. The product is a set of vectors that is provided to NRL, along with the radar observations, up to three times a day. These state vectors are processed at NRL using Special-K orbit determination software¹⁷ to produce a set of ephemerides. These ephemeris files are reformatted into the consolidated prediction format (CPF)¹⁸ used by the ILRS tracking stations. This format consists of minute satellite state vector (x, y, and z positions and velocities at a given time plus other parameters) over the several day prediction period. These predictions are distributed via the NASA CDDIS data center and the European Data Center.

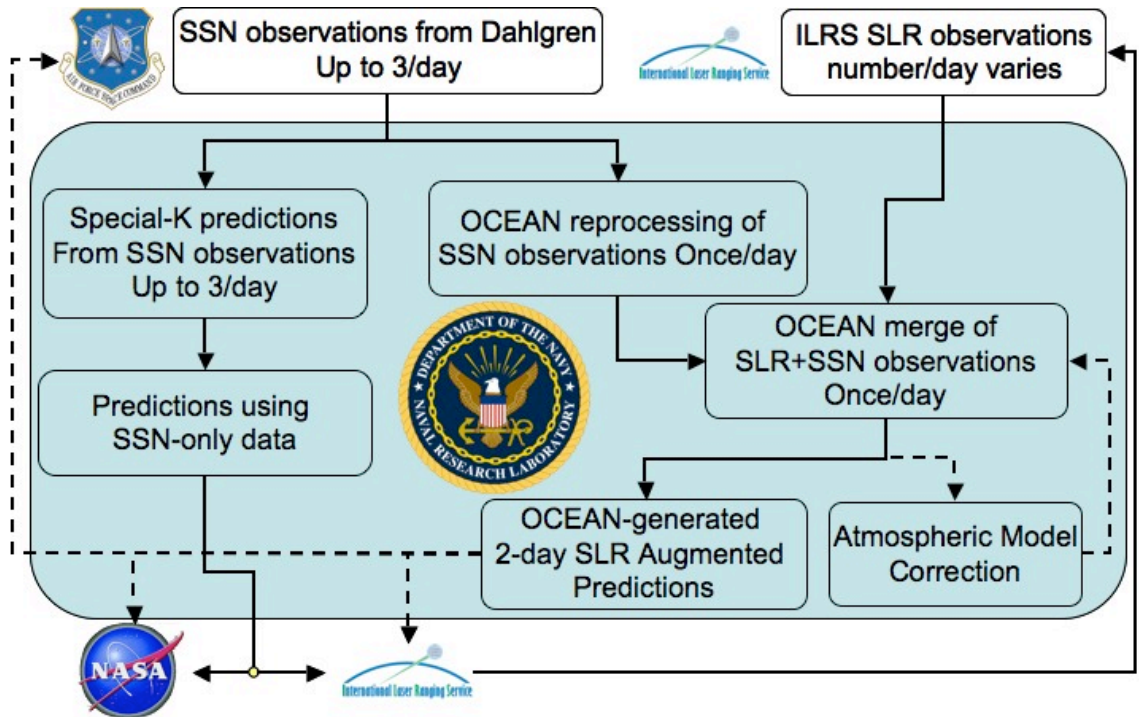


Figure 5 A schematic of the data flow and processing of ANDERR observations

A set of predictions is also computed once per day using the NRL Orbit Covariance Estimation and Analysis (OCEAN)¹⁹ orbit determination code. The radar observation data is merged with the SLR observation data and processed by OCEAN to generate a 2-day SLR augmented set of predictions. Figure 5 depicts the two data flow processes.

DATA PROCESSING AND ANALYSIS

Version 5.01 of OCEAN was configured to make weighted least squares estimates of the initial conditions and the scale factor for the drag model. The observation data were sampled at 48 hour intervals (beginning in the middle of a day) and the fit and prediction final ephemeris was produced. The observation data were corrected for known biases (and center of mass) and weighted using past sensor performance values so that the SLR data naturally biases the solutions toward reality in the hybrid SSN and SLR runs. The high fidelity force models including either EGM-96 or GGM02C at degree and order 70x70, the ocean tides, the MSIS density models, the HWM93 thermospheric winds, and all IERS conventions frames and displacement typical for accurate SLR processing.

A comparison between the resulting MAA C_D and FCal C_D from the OCEAN run, using NRL MSISE2000 and a priori area and mass information, yields very little difference between the two objects as seen in Figure 6. The average C_D value for MAA is 1.690 with a standard deviation of 0.1557. The average

C_D value for FCal is 1.676 with a standard deviation of 0.1703. These results are clearly non-physical as seen from Eq. 1, as the value is well below 2.0. The MSIS2000E model is over-estimating the atmospheric density by about 25% on average and the OCEAN code is correcting for this by scaling the B term down. This over-estimation of the thermospheric density is in direct agreement with the findings of Emmert and Picone²⁰. The average ratio for MAA is 80.2% with a standard deviation of 7.46% and the average ratio for FCal is 79.5% with a standard deviation of 8.1%.

The observations were also processed using the Jacchia 70 (J70) model atmosphere. The results are plotted against the MSIS results in Figure 7. The average C_D value for MAA_{J70} is 1.727 with a standard deviation of 0.2483. The average C_D value for $FCal_{J70}$ is 1.720 with a standard deviation of 0.2755. The average value is closer to theory but the scatter is 59% larger for the MAA and 62% larger for FCal when using J70 instead of NRL MSISE2000.

The primary drivers of the atmosphere are solar radiation heating and geomagnetic heating. These drivers have inputs into MSIS and J70 in the form of the F10.7 cm radio flux, a proxy (due to its ease of measurement on the ground) for the solar ultraviolet flux that heats the atmosphere. The ap and kp indices are a measure of geomagnetic activity at the Earth and are used by atmospheric models to drive the geomagnetic heating in the atmosphere. Figure 8 plots the OCEAN fitted C_D values against both the daily F10.7 cm flux and the daily index. There is a slight trend with the F10.7 cm flux values, which may be indicative that the temperature in the atmospheric models is incorrect and over-estimating the atmospheric density. There is clear correlation that the geomagnetic activity, even at these relatively low levels of geomagnetic activity, is not being completely accounted for in the MSIS or J70 models. Latency in the C_D values with response to the geomagnetic activity is expected (and observed) due to the timescales that the atmosphere responds to the geomagnetic forcing.

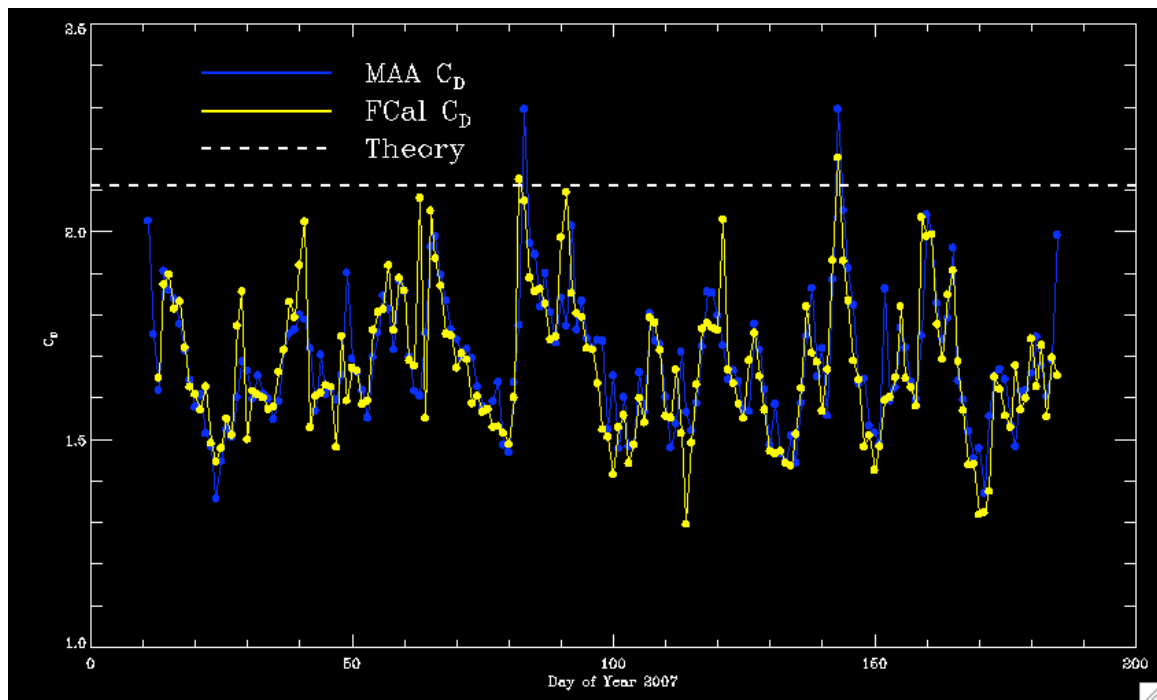


Figure 6 OCEAN fitted C_D values, using NRL MSISE2000 for the MAA (blue) and FCal (yellow) spacecraft.

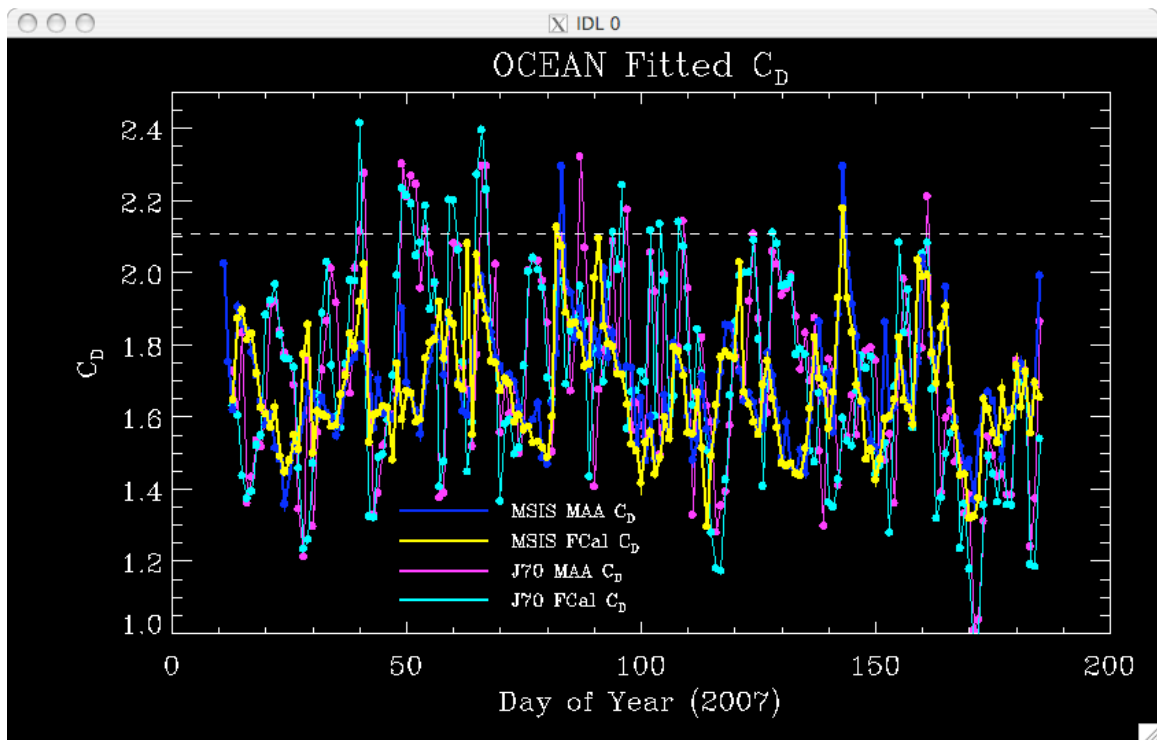


Figure 7 OCEAN fitted C_D values, using NRL MSISE2000 for the MAA (blue) and FCal (yellow) spacecraft; using NRL Jacchia 70 for the MAA (purple) and FCal (light blue) spacecraft.

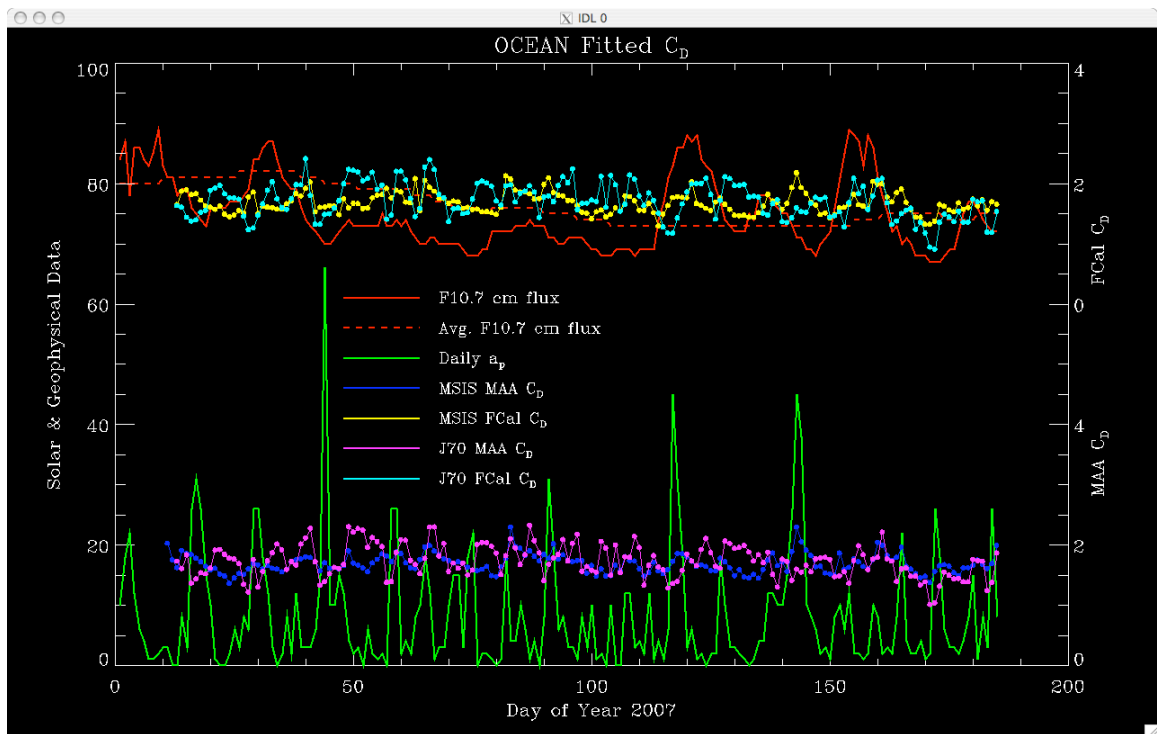


Figure 8 OCEAN fitted C_D values are plotted (right hand scale) with the solar f10.7 cm flux and the daily average A_p geomagnetic index.

For fit-spans that are much longer than the timescale of an objects variations in B one can state the relationship between two objects i and j as

$$\frac{B_i^T}{B_j^T} = \frac{B_i^M}{B_j^M} \quad (5)$$

where B^T represents the true value of B and B^M is the modeled, or fitted, value. Due to the inherent symmetry of the ANDERR spacecraft, the frontal area (A) is well characterized and remains constant independent of orientation and the mass (m) is constant for both the ANDERR MAA and the FCal spacecraft. Hence, Eq. 5 may be re-written as

$$B_i^T = B_i^M \frac{C_{Dmaa}^T}{C_{Dmaa}^M} \quad (6)$$

using the ratio of MAA C_D values, true over modeled, as a calibration correction which can be applied to obtain B^T of an independent object i .

The practical impact of having a correctly scaled thermospheric density was measured by comparing the 24-hour prediction revolution to the reference ephemeris. This was constructed by establishing a time series of scale factors required to rescale the recovered C_D from the OCEAN fit using the MSIS atmospheric model over a 3 day fit interval on the MAA spacecraft. These scale factors were applied to each unique day (multiple scalings occur during the testing fit and prediction interval) and do include scaling on the prediction interval (posterior knowledge was utilized).

The comparison is a measure of the in-track bias measured over one orbit period at the end of the first day of prediction. This is constructed from time of day and not last dataset, and may be measuring more than just a 24 hr prediction, as the observation data is not uniformly available on a target of this altitude. Both the FCal and the MAA were generated with this process (using the MAA's rescale factor)

A comparison of the in-track time bias, the time difference between where the predicted object location and the actual location, is used as a performance metric for three different OCEAN fits using NRL MSISE2000 as the atmospheric model. Three cases were processed for FCal using information from a 48-hour fit of MAA as the reference object. First the FCal data were processed allowing the B term to float, or be scaled by OCEAN. The second case was to fix the B term to the theoretical value using 2.1088 as the C_D . The third process scaled the B term as described by Eq. 6. The results are plotted as Figure 9 at the 24-hour mark and the means and standard deviations are presented in Table 1. Using the daily MAA scale factors shows a marked improvement in the mean (15.2%) and the standard deviation (39.9%) over the reference method.

Table 1. FCal In-Track Time Bias (msec)

	Reference	Theory	Scaled Fixed	Scaled Daily
Mean	35.43	202.82	45.40	30.05
Std. Dev.	47.33	200.49	53.69	28.46

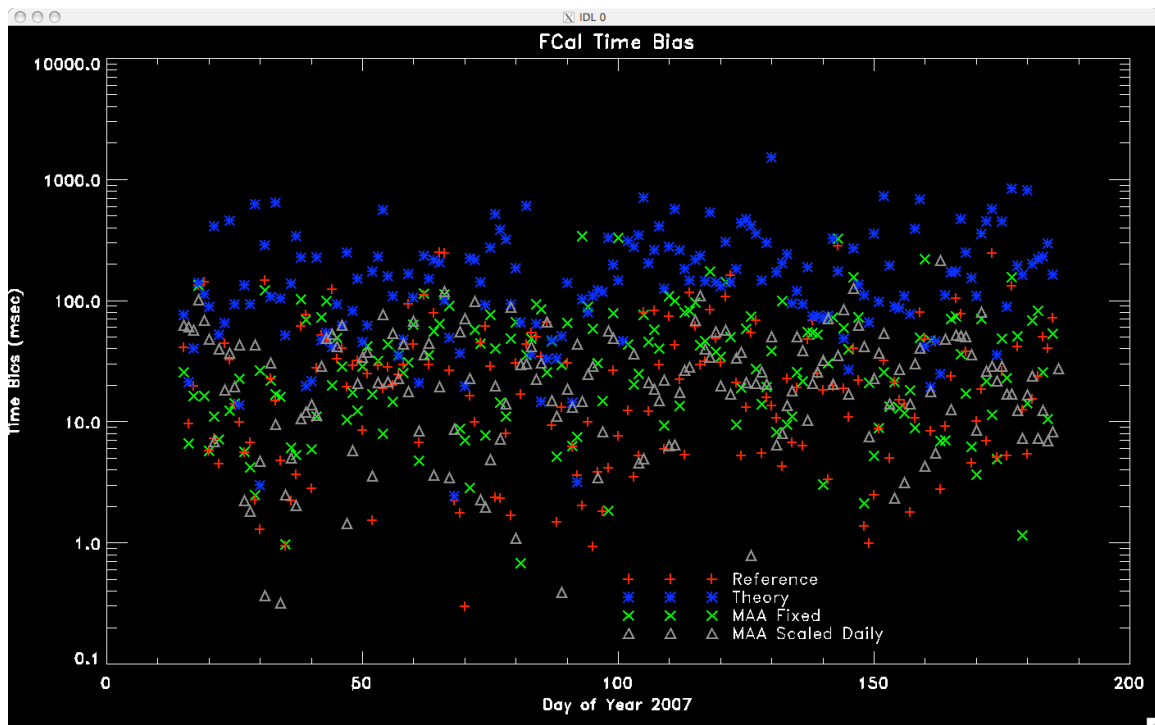


Figure 9 In-track time bias of the FCal spacecraft predictions at 24 hours. Allowing B to float (red), Fixing B to theory (blue), scaling B with average MAA results for the 6-months (green), scaling B with daily MAA results (grey).

CONCLUSIONS

It is clear that the ANDERR spacecraft are useful calibration targets due to their well-characterized size and shape. The SLR observations performed by the members of the ILRS have been used to augment the radar data to constrain the accuracy and stability of the estimated ballistic coefficient and to assess the accuracy of the predictions with absolute confidence. The data show a consistent over estimation of the density by the atmospheric models, NRLMSISE 2000 as well as J70. The average in-track time bias at the 24-hour mark improved by 15.2% with a 39.9% improvement in standard deviation. While the average fitted C_D for J70 was closer to the analytic value, the MSIS C_D values have considerably less variation. The over specification of total density is in agreement with the findings of Emmert and Picone²⁰, who have shown a consistent decrease in thermospheric density of the past three decades. The models are having a difficult time properly capturing the effect of geomagnetic forcing (especially at low end of the solar/geomagnetic forcing range), as correlations are evident in the fitted C_D values with the geomagnetic a_p index. The ANDERR data set is extensive and the objects are not expected to decay until December, 2007 (MAA) and April 2008 (FCal). We expect to continue this work over the entire mission duration, and apply the corrections to other objects. Work will also focus on short arc studies, $\frac{1}{4}$ to $\frac{1}{2}$ of an orbit where geometric solutions have been collected.

FUTURE FLIGHTS

Atomic oxygen (O), the major constituent of the Earth's thermosphere above 200 km altitude is both a driver and a tracer of atmospheric motions in the thermosphere and plays a pivotal role in interactions with the ionosphere through ion-drag and chemical reactions. Satellites in low-Earth orbit require knowledge of O densities to address engineering issues in low-Earth-orbit missions. The major difficulties in O measurements involve ambiguities due to the recombination of O in the sensor surfaces to yield O_2 , which is then measured with a mass spectrometer; similar difficulties exist for atomic hydrogen H and nitrogen N.

A follow-on ANDE mission is scheduled for April 2009. This mission will consist of two 19-inch diameter spherical spacecraft, each fitted with retro-reflectors. One of the spacecraft will carry onboard instrumentation designed to simultaneously measure thermospheric density, composition and winds at the spacecraft location. This new miniaturized charged particle spectrometer is capable of measuring relative densities and energies of the neutral and ion constituents in the upper atmosphere. Neutral atoms are ionized before striking internal surfaces and accommodated atoms and molecules are discriminated from incident ones according to their energies. The ion source sensitivity is about 1.3×10^{-4} /s per microAmp electron beam current for a number density of $1/\text{cm}^3$; operating with 1 mA emission (about 0.2W cathode power), signals of 100/s with integration period of 1 second correspond to a neutral atom density of about $10^3/\text{cm}^3$ with 10% variance. Total power for the spectrometer is less than 0.5 W with a mass of about 0.5 kg.

The active spacecraft will also carry an optical communications experiment. The NRL modulating retro-reflector (MRR) system consists of an optical retro-reflector coupled with a multiple quantum well (MQW) electro-optic shutter^{21,22}. When a low voltage (on the order of 5V) is applied to the MQW device, the shutter is open allowing photons from the interrogation beam to enter the system. The photons are then reflected back along the original angle of incidence by the retro-reflector. The electronic driver encodes the data to be transmitted, which is modulated by the MQW device, resulting in a modulated return beam carrying the data stream. This system provides a compact, low power (<50 mW per device), asymmetric optical communication platform. The Field-of-View (FOV) of a typical mounted device is of the order of 26 degrees (far field) and the operation wavelengths for the NRL units can be 980 nm or 1.06 μm , or 1550nm. The active sphere will have a predetermined pattern of MRRs distributed over the sphere. For this experiment, the system's nominal data transmission rate will be between a few bits per second and ~10 kbps. The ground site intended for use in the MRR communications experiment is the NRL Midway Research Center in near Quantico, VA.

REFERENCES:

1. A.C. Nicholas, et al., "The Atmospheric Neutral Density Experiment (ANDE)" Proceedings of the 2002 AMOS Technical Conference, Maui HI, Sept. 2002.
2. A.C. Nicholas, G.C. Gilbreath, S.E. Thonnard, R.A. Kessel, R. Lucke, C.P. Sillman. "The atmospheric neutral density experiment (ANDE) and modulating retroreflector in space (MODRAS): combined flight experiments for the space test program" Proc. SPIE Vol. 4884, p. 49-58, Optics in Atmospheric Propagation and Adaptive Systems V; Anton Kohnle, John D. Gonglewski; Eds., March 2002.
3. A. Nicholas, S. Thonnard, I. Galysh, P. Kalmanson, B. Bruninga, H. Kelly, S. Ritterhouse, J. Englehardt, K. Doherty, J. McGuire, D. Niemi, H. Heidt, M. Hallada, D. Dayton, L. Ulibarri, R. Hill, M. Gaddis, B. Cockreham, "An Overview Of The ANDE Risk Reduction Flight", Proceedings of the AMOS Technical Conference, Maui, HI., Sept. 2002.
4. D. Vallado, and S. Carter, "Accurate Orbit Determination from Short-Arc Dense Observational Data", Paper AAS 97-704, AAS/AIAA Astrodynamics Specialist conference, Sun Valley, Idaho, Aug 4-7, 1997.
5. L. Jacchia, "New Static Models of the Thermosphere and Exosphere with Empirical Temperature Profiles," *Smithsonian Astrophys. Observatory Special Rep. No. 313*, May 6, 1970.
6. A. E. Hedin, "MSIS-86 Thermospheric Model," *J. Geophys. Res.*, *92*, 4649-4662, 1987.
7. A. E. Hedin, "Extension of the MSIS Thermosphere Model Into the Middle and Lower Atmosphere," *J. Geophys. Res.*, *96*, 1159-1172, 1991.
8. J. M. Picone, A. E. Hedin, D. P. Drob, and A. C. Aikin, "NRLMSISE-00 Empirical Model of the Atmosphere: Statistical Comparisons and Scientific Issues," *J. Geophys. Res.*, (2001).

9. Cox, C.M., and F.G. Lemoine, Precise Orbit Determination of the Low Altitude Spacecraft TRMM, GFZ-1, and EP/EUVE Using Improved Drag Models, Paper AAS 99-189, presented at the AAS/AIAA Space Flight Mechanics Meeting, Breckenridge, Colorado, February, 1999.
10. Knechtel, E.D., and W.C. Pitts, Normal and Tangential Momentum Accomodation for Earth Satellite Conditions, *Astronautica Acta*, Vol. 18, 1971
11. A. E. Hedin, E. L. Fleming, A. H. Manson, F. J. Schmidlin, S. K. Avery, R. R. Clark, S. J. Franke, G. J. Fraser, T. Tsuda, F. Vial, and R. A. Vincent, "Empirical Wind Model for the Upper, middle and Lower Atmosphere", *J. Atmos. Terr. Phys.*, 58, 1421-1447, 1996.
12. Fredo, R.M., A numerical Procedure for Calculating the Aerodynamic Coefficients for Complex Spacecraft Configurations in Free-Molecular Flow, Master's Thesis, Department of Aerospace Engineering, Pennsylvania State University, August 1980.
13. A.C. Nicholas, T. Finne, M. A. Davis, "Atmospheric Neutral Density Experiment Risk Reduction (ANDE-RR) Flight Hardware Details", http://ilrs.gsfc.nasa.gov/docs/anderr_hw.pdf, 2007.
14. Bird, G. A., "Molecular Gas Dynamics and the Direct Simulation of Gas Flows", Oxford University Press, page 172, 1994.
15. Lumpkin, F. Private communication, NASA JSC, 2007.
16. Pearlman, M.R., Degnan, J.J., and Bosworth, J.M., "The International Laser Ranging Service", *Advances in Space Research*, Vol. 30, No. 2, pp. 135-143, July 2002.
17. S. Coffey, H. Neal, C. Visel, P. Conolly, "Demonstration of a Special-Perturbation-Based Catalog in the Naval Space Command System", *Proceedings of /AAS/AIAA Space Flight Mechanics Meeting, Monterey, February 1998.*
18. Ricklefs, Randy, https://ilrs.gsfc.nasa.gov/docs/cpf_1.01.pdf
19. M. Soyka, J. Middour, P. Binning, H. Pickard, J. Fein, "The Naval Research Laboratory's Orbit / Covariance Estimation and Analysis Software: OCEAN", *Proceedings of AAS/AIAA Astrodynamics Meeting*, pp1567 - 1586, Sun Valley, Idaho, 1997.
20. Emmert, J. T., J. M. Picone, J. L Lean, and S. H. Knowles, Global change in the thermosphere: Compelling evidence of a secular decrease in density, *J. Geophys. Res.*, 109, A02301, doi:10.1029/2003JA010176, 2004.
21. G. C. Gilbreath, W. S. Rabinovich, T. J. Meehan, M. J. Vilcheck, R. Mahon, Ray Burris, M. Ferraro, I. Sokolsky, J. A. Vasquez, C. S. Bovais, K. Cochrell, K.C. Goins, R. Barbehenn, D. S. Katzer, K. Ikossi-Anastasiou, and Marcos J. Montes, "Large Aperture Multiple Quantum Well Modulating Retroreflector for Free Space Optical Data Transfer on Unmanned Aerial Vehicles", *Opt. Eng.*, 40 (7), pp. 1348-1356.
22. G.C. Gilbreath, S.R. Bowman, W.S. Rabinovich, C.H. Merk, H.E. Senasack, "Modulating Retroreflector Using Multiple Quantum Well Technology", U.S. Patent No. 6,154,299, awarded November, 2000.